Meningiomas Assessed with In Vivo 3D ^{1}H-Magnetic Resonance Spectroscopy Integrated Into a Standard Neurosurgical Image Guidance System: Determining Biochemical Markers of Clinically Aggressive Behavior and Providing a Resection Advantage

A Thesis submitted to The University of Arizona College of Medicine-Phoenix in partial fulfillment of the requirements for the Degree of Doctor of Medicine

Nina Zobenica Moore, MSE

2011

Dedicated to my husband for his support throughout my long endeavor to become a neurosurgeon and complete this research.

Acknowledgements

A special thanks to the team of people that helped this project progress to this point:

To Robert Ryan and Michelle Carle for helping with the leg work for the project during their time here at BNI from Alberta, Canada.

To Berkay Kanberoglu, Josef Debbins and Sharmeen Jooman for their help getting the MR Spectroscopy scans and STEALTH overlay ready.

To John Karis and Tejas Sankar who provided support of our project and intellectual input.

To Nikolay Martirosyan who ran to the operating room when I could not get there to collect the samples.

To Jennifer Eschbacher who read all of the pathology and immunohistochemical slides.

To the pathology lab department for their help making the slides and to the NMR staff and Brian Cherry over at ASU for their help with the HR-MAS spectra collection.

To the neurosurgery team at Barrow Neurological Institute. In particular I'd like to thank the neurosurgical secretaries Michelle and Valerie for helping with the pre-op preparations.

To the neurosurgery residents who were instrumental in tissue collection.

To the neurosurgeons Dr. Robert Spetzler, Dr. Peter Nakaji, Dr. Randall Porter and Dr. Kris Smith for their help in patient enrollment, intellectual input and tissue collection.

Finally, to Dr. Mark Preul for his tremendous support and insight into MR Spectroscopy and meningiomas.

Abstract:

Introduction: Using *ex vivo* nuclear magnetic resonance spectroscopy (NMR) of resected meningioma tissue, we have previously shown that meningiomas are made up of biochemically heterogeneous regions, and that the quantities of various biochemical markers are correlated to specific genetic markers of aggression. In this study we tested the hypothesis that *in vivo*, multivoxel, three-dimensional proton magnetic resonance spectroscopic imaging (3D ^{1}H-MRSI) can—non-invasively—detect more aggressive regions within individual meningiomas.

Methods: Multivoxel 3D ^{1}H-MRSI was performed pre-operatively on 15 usable patients with recurrent or newly diagnosed meningiomas using a 3T GE Signa scanner. Quantified spectral metabolite peaks were used to select voxels that had high or low alanine for tissue sampling. 3D ^{1}H-MRSI was integrated into a standard image guided surgery (IGS) system; a mask of the voxel was loaded onto the IGS system allowing surgeons to precisely extract tissue intraoperatively according to biochemical mapping. *Ex vivo* NMR and conventional histological grading were performed on the extracted tissue.

Results: Tumor spectra showed biochemically heterogeneous regions, especially for choline, lactate and alanine. Mean alanine concentrations were lower in more aggressive--histologically and immunohistochemically--regions of the meningiomas in the study. In addition, lower grade meningiomas showed high alanine at the tumor periphery with decreased central alanine. *Ex vivo* NMR was well-correlated with *in vivo* 3D ^{1}H-MRSI.

Conclusions: Non-invasive detection of various intratumoral biochemical markers using 3D 1H-MRSI can distinguish areas within meningiomas that express more aggressive features. There is regional heterogeneity in the concentrations of these markers within individual tumors. Furthermore, 3D 1H-MRSI may be able to exploit these regional differences to separate more aggressive from less aggressive areas within a given meningioma. Such knowledge may be useful to

the neurosurgeon faced with the task of meningioma resection, and in the planning adjuvant therapy for residual meningioma tissue following subtotal removal.

Table of Content:

List of Figures and Tables

Background

Meningiomas originate from arachnoidal cap cells and comprise over one-third of all primary brain and central nervous system tumors.[27,37] The World Health Organization (WHO) classifies meningiomas into three grades: benign (grade I), atypical (grade II), and anaplastic or malignant (grade III). Treatment differs based on grade and behavior of meningiomas. Suspected grade I meningiomas can be followed with serial imaging and resected surgically if they show growth or begin to cause mass effect. In pathologically proven grade I meningiomas, gross total resection (GTR) is thought to be curative, and no adjuvant treatment is offered. Grade II or III meningiomas are commonly thought to require adjuvant therapy following aggressive resective surgery in order to prevent regrowth and local recurrence. The three meningioma grades are assigned based on universal histological markers, including the presence and number of mitotic figures, overall cellularity and growth pattern, nuclear-to-cytoplasmic ratio, nucleoar prominence, and presence of necrosis.[4] Though the majority of meningiomas are benign grade I tumors, 23-24% of the tumors are atypical (Grade II) and 1-3% are found to be anaplastic (Grade III) under the new WHO classification system.[34,40]

However, even supposedly benign meningiomas are heterogeneous, exhibiting a variety of different biological features and demonstrating clearly aggressive behavior in some cases.[23-26] In fact, the five-year recurrence rate is 12% for grade I meningiomas which have undergone gross total resection (GTR)—again, thought to be curative—and 41% for atypical tumors having undergone GTR.[22] The five-year survival rate for benign meningiomas is 90-91% in patients less than 44 years old[13,17], dropping to 78% with atypical and 65% with anaplastic histology in the same age group. [17]

Given the percentage of recurrent "benign" meningiomas, histology may not be the best measure of aggression. Immunohistochemical markers, such as the MIB-1 proliferation index, and genetic markers, namely deletion of chromosomes 1p and 14q, and deletion or trisomy of chromosome 22q, may be better measures of aggressive behavior.[1,7,11,14,20,24,25] Still, these tests can only be done after resected or biopsied tumor tissue has been obtained by surgery. Furthermore, meningiomas show considerable intratumoral regional heterogeneity of these markers, leading to possible sampling error during biopsy with the potential for underestimating tumor aggression. Consequently, having the ability to identify an aggressive

meningioma—or more aggressive portions of a meningioma—preoperatively, is an important goal. Such information might allow surgeons to plan more extensive resective surgery or consider the use of up-front adjuvant radiation in patients whose tumors are more likely to recur. It might also be useful in highlighting key regions of the tumor which should be biopsied when complete resection is unsafe or technically prohibitive. Finally, and no less important, it might contribute to a better understanding of the biology, growth, and behavior of meningiomas, which historically have represented a tumor group that has received less attentive research compared to gliomas.

Proton magnetic resonance spectroscopic imaging (^{1}H-MRSI) can be used to diagnose, *in vivo*, the basic histologic types of many common brain tumors by identifying their characteristic biochemical markers.[15,23,24,28,29,31,32] Meningiomas are globally characterized by a high alanine peak that differentiates them from other intracranial neoplasms, and in addition are the first brain tumor type wherein biochemical data from MRS has been linked to chromosomal and genetic information.[24,26,28,29] The magnitude of the alanine resonance appears to be associated with variations in meningioma metabolism that have biological significance. Recent e*x vivo* nuclear magnetic

resonance (NMR) analyses of meningioma tissue showed a negative correlation between alanine concentrations and recurrence, with tumor grade, and with gene and chromosomal aberrations.[23-26] Further work has shown that the spectral characteristics of meningiomas, including the presence and concentration of alanine, seen using *in vivo* ^{1}H-MRSI are well-correlated with findings on *ex vivo* high resolution magic angle spinning nuclear magnetic resonance (HR-MAS).[36] However, what has not yet been shown is whether *in vivo* ^{1}H-MRSI can accurately determine regional variations in alanine and other metabolites within a given meningioma, and further whether these regional variations meaningfully predict more aggressive areas of the individual tumor verified by *ex vivo* MRS, histology, immunohistochemistry or genetic analysis. *In vivo* multi-voxel 3D proton magnetic spectroscopic imaging (3D 1H-MRSI) provides a means of accomplishing this, because it allows for the quantification of metabolites in several individual voxel units which can cover the entire volume of a tumor. These voxel units can then be co-registered into a standard neurosurgical navigation system to allow for the targeted selection of tissue sample sites.

In this paper, we report on a series of patients with newly diagnosed and recurrent meningiomas in whom *in vivo,* multi-voxel 3D ^{1}H-MRSI scans covering the tumor were acquired preoperatively. In these patients, spectroscopic data were co-registered to standard anatomical MRI scans and integrated into a standard intraoperative image guided surgery (IGS). Image-guidance was used prospectively to obtain biopsy specimens from pre-selected intratumoral regions characterized by variations specifically in alanine and choline. Other resonances from prominent metabolites were also examined post-operatively. The resulting specimens were analyzed using *ex vivo* MRS and standard histology (including MIB-1 index) and the findings correlated with preoperative *in vivo* MRS data. We sought to demonstrate that the biochemical information from non-invasive *in vivo* 3D 1H-MRSI was a logical translational application of previous ex vivo MRS meningioma studies and, further, that targeting tumor tissue regions based on the resonance intensity mainly of alanine can identify meaningful areas of metabolic and histologic characteristics that connote increased aggression or malignant behavior within meningiomas.

Methods

Patients

Twenty-seven consecutive patients with an intracranial tumor consistent with meningioma on routine diagnostic imaging were selected prospectively at the Barrow Neurological Institute of St. Joseph's Hospital and Medical Center for a preoperative 3D ^{1}H-MRSI scan if: 1) there was suspicion by neurosurgeons and neuroradiologists that the intracranial mass was a meningioma; and 2) if at least a portion of the mass was suitable for spectroscopic analysis, i.e., was large enough to contain multiple 3D ^{1}H-MRSI voxels fully within the tumor without partial volume. 3D 1H-MRSI was done at the end of the routine MRI sequence for STEALTH (Medtronic, Minneapolis, MN) IGS navigation.

Of the 27 patients selected for pre-operative scanning, 15 patients had meningiomas with usable spectra from whom tissue samples were collected (Table 1). 27 of the 30 samples from the 15 patients had tissue analyzed using *ex vivo* HR-MAS. 27 of the 30 samples from 13 patients had complete immunohistochemical and histological analysis done on voxel tissue. Of the remaining 14

patients, 3 did not harbor meningiomas, 2 were severely claustrophobic and would not enter the 3T magnet, 1 moved his head during the scan, 2 did not undergo surgery, and 4 did not have usable spectra due to problems with water suppression or difficulties with 3D 1H-MRSI region of interest (ROI) placement.

3D ^{1}H-MRSI Acquisition and Processing

Routine preoperative MR scans as well as the multivoxel 3D ^{1}H-MRSI were performed on a 3T GE Signa scanner (General Electric Healthcare, Waukesha, WI). Preoperative axial T1 wand scans with gadolinium contrast were performed for IGS co-registration. These were used as an anatomical guide in placing the 3D ^{1}H-MRSI ROI. A 3D ^{1}H-MRSI ROI was placed covering the entire tumor in the axial, sagittal and coronal views avoiding unnecessary areas of bone while including normal brain within the ROI. The ROI included a grid of 9x9 voxels per slice and 7 slices resulting in a total of 567 voxels. ROI boundary lines intersect within the perimeter voxels making the spectra unreliable and thus leaving a total of 343 usable voxels. The field of view (FOV) was standardized to 7.0 with a slice thickness of 7mm and a total volume thickness of 42mm, resulting in voxels of

about 1 ml of tissue volume. Additional acquisition parameters that were used included: an inter-pulse delay (TR) of 2000 ms and a spin-echo refocusing time (TE) of 144 ms.[15] Higher order shim (HOS) was performed prior to 3D ^{1}H-MRSI acquisition in zoom mode with placement of the HOS ROI over the entire brain. HOS was performed until the actual RMS value was within 0.5 of the predicted RMS value. The HOS scan length was 9 seconds and was usually repeated once to improve values. The 3D ^{1}H-MRSI prescan was then run and accepted when the line width was below 20. The acquisition of 3D ^{1}H-MRSI took 9 to 15 minutes including calibration scan, 3D 1H-MRSI ROI placement, and HOS. The entire study, including the routine MRI sequence for STEALTH IGS, lasted about 20 to 29 minutes. 1D ^{1}H-MRSI scans were performed on the last few subjects prior to 3D ^{1}H-MRSI acquisition to compare spectra. An interpulse delay (TR) of 1500ms and a spin-echo refocusing time (TE) of 144ms were used for these acquisitions.

Functool Software (GE Systems) images were generated to verify the quality of the spectra immediately post scan. Due to the limited processing capabilities of the Functool software, 3D ^{1}H-MRSI data files were exported to a SUSE Linux computer station where the

files were processed using GE SAGE software (V7, GE Medical Systems, Milwaukee, WI). The data underwent convolution from the frequency domain to the time domain. LCModel (V6.2-0, Provencher) software was then used to quantify spectral metabolite peaks. 3D ^{1}H-MRSI requires a GE SAGE/LCModel interface designed by McClean.[18] The spectra were analyzed using the following parameters: ppm range of 0.2ppm to 4.0ppm, calibration factor of 1, SDDEGZ 999.0, SDDEGP 1.0, and basis set specific for the 3T scanner TE 144. Individual voxel spectra were output into separate files.

29	**PATIENTS SCANNED**	
	18	primary meningiomas with tissue collected
	1	recurrent meningioma with tissue collected
	3	not meningiomas
	1	moved head during MRS acquisition
	2	severely claustrophobic
	2	no operation
19	**3-D ^{1}H-MRS data sets examined with SAGE/LCModel**	
	15	sets with quantifiable metabolites, areas of interest identified within tumor and selected for resection
	4	sets discarded – inadequate water suppression or voxel placement prevented analysis

Table 1: Summary of Patient Scans

LCModel quantifies the resonance intensity of the following metabolites: choline at 3.2 ppm, creatine at 3.0ppm, NAA at 2.0 ppm, alanine at 1.47 ppm, lactate at 1.3 ppm, and lipids between 1.3 ppm and 0.9ppm. Particular interest was given to alanine concentrations in individual tumor voxels. LCModel recommendations on data

interpretation were used. A %SD < 20% was used as a rough criterion for estimates of acceptable reliability. Averages over a group of LCModel analyses of similar spectra can significantly reduce the uncertainties in cases where %SD was higher than 20%.

Co-Registration of 3D ^{1}H-MRSI and MRI

The selection of voxels of interest and creation of a 3D ^{1}H-MRSI overlay for the STEALTH IGS was fully automated using in-house code written in MATLAB (Mathworks, Natick, MA). 3D ^{1}H-MRSI unprocessed data files contain the coordinates of the ROI voxel grid. The coordinates were extracted from this file and were used to coregister voxel locations with the T1 axial image. Metabolite concentrations from LCModel for each voxel were used to generate alanine and choline metabolite maps representing voxel areas of high and low concentrations. Voxels containing the maximum and minimum alanine concentrations within the tumor were marked using the software and the overlay was generated as a series of DICOM images. The two highest alanine concentration voxels were marked and two of the lowest alanine concentration voxels were marked with

the automated program. The alanine resonance distribution was targeted prospectively because of its previously identified unique implication in meningioma metabolism.

Integration of 3D 1H-MRSI into an Image Guided Surgery (IGS) System

A copy of axial T1 images with gadolinium and the 3D ^{1}H-MRSI overlay images were loaded into the STEALTH IGS. The overlay was assigned a transparency where the voxels were illuminated in green and superimposed on the axial images while still allowing tumor anatomy to transmit through the overlay. During surgery, the transparency could be adjusted to show the overlay during tumor resection. The merged images were visualized in a standard tri-planar display.

Integration of the 3D ^{1}H-MRSI data into the STEALTH IGS (Figure 1) successfully allowed for pre-surgical selection of voxels for spectral and tissue analysis. Knowledge of the areas of interest was easily conveyed to the surgeon before and during the operation by the color overlay showing the regional distribution of selected resonances

viewed on the IGS. Neurosurgeons collected the tissue from the locations marked on the STEALTH IGS prior to excision of the tumor to preserve spatial orientation of the tissue using the STEALTH probe to define the boundaries. In smaller tumors, at least two samples were obtained from targeted areas with the neurosurgeon determining what remaining tumor needed to be sent to histology. Samples were immediately preserved in formaldehyde for histological analysis or snap frozen in liquid nitrogen for later *ex vivo* NMR analysis.

Spectral confirmation and spatial correlation of 3D ^{1}H-MRSI information and the IGS system were demonstrated by comparing *ex vivo* tissue spectra, the *in vivo* spectra, and histological results, as well as previous work with phantoms and co-registration and integration of MR imaging techniques into the STEALTH IGS system (Kanberoglu, et al. unpublished data).

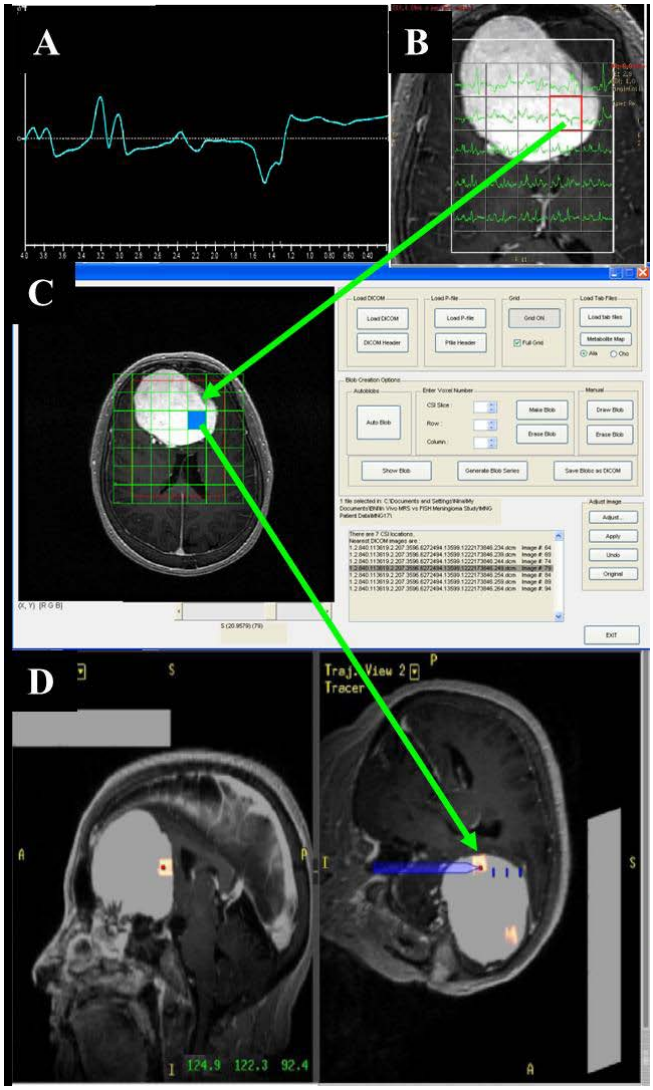

Figure 3: Voxel selection and Image Guidance System (IGS) Overlay. A) Selected 3D ^{1}H-MRS spectra generated from LCModel software. B) Overlay from GE Scanner Functool software with chosen voxel highlighted in red. C) GE Sage/LCModel processed spectra data incorporated into overlay program coded with MATLAB software where the chosen voxel is highlighted in blue. D) Overlay from MATLAB program placed into image guidance system showing targeting of voxel tissue.

Histologic Analysis and ex vivo HR-MAS NMR

Thirty-five tissue samples were harvested with 27 tissue samples usable for histological, immunohistochemical, and further *ex vivo* high resolution-magic angle spinning (HR-MAS) NMR analysis. The remaining samples were either saved for later genetic analysis due to small tissue quantity or were not used altogether due to poor tissue quality from electrocautery use. One third of the tissue in each sample was fixed, embedded and stained with the MIB-1 marker Ki-67 and hematoxylin and eosin (H&E). Both stains are the standard for pathological grading of meningiomas. A neuropathologist, blinded to imaging data and patient information, analyzed each sample, describing the histological characteristics, assigning a MIB-1 percentage, and grading the sample according to WHO criteria.

HR-MAS NMR was performed at the Magnetic Resonance Research Center at Arizona State University. A volume (~0.3ml) from each tissue sample was evaluated *ex vivo* by HR-MAS NMR as solid tissue suspended in 4mm Bruker MAS rotor inserts with deuterium oxide. Spectra were acquired with a Bruker 400MHz (9.4T) Combine Liquid/Solids NMR at 4^{o}C and with a T_2-filtered Carr-Purcell-

Meiboom-Gill (CMPG) pulse sequence. Spectra were processed using Chenomx NMR Suite version 7.0 (Chenomx Inc.). HR-MAS spectra were compared quantitatively with the *in vivo* 3D ^{1}H-MRSI spectra using a Pearson correlation between metabolite concentrations for each set of voxel spectra. Concentrations from alanine, lactate, creatine, choline, NAA and myo-inositol were compared. This technique was used both to validate the 3D ^{1}H-MRSI spectra as well as the accuracy of sampling using the STEALTH IGS overlay.[2,6,12, 19, 30,41]

Statistical Analysis

Metabolite datasets from the biopsied tissue were analyzed with respect to clinical and pathological factors. Metabolite distribution was compared within the ROI, such as in the periphery versus concentrations centrally. The periphery consisted of the outermost voxels within the tumor in the 3D volume—the outer shell of the tumor. Central voxels were considered those within the tumor not contacting the edge of the tumor—the core of the tumor. The mean Ala concentration across the maximum Ala voxels selected for biopsy were compared between the aggressive and non-aggressive tumor groups using a two-tailed, independent samples t-test, assuming unequal

variance. Scatterplot and Pearson Correlation analysis were used to analyze all the targeted alanine metabolite concentrations with regard to MIB-1%. Creatine, choline, lactate, NAA, glutamine, glutamate and myo-Inositol mean concentrations from the maximum alanine containing voxels were compared between the aggressive and non-aggressive tumor groups using a two-tailed, independent samples t-test, assuming unequal variance as well as MIB-1% using the Pearson Coefficient. Peripheral metabolite concentration to central metabolite concentration were compared using a two-tailed, paired distribution t-test.

Results

Subject	Meningioma Subtype	Grade	Recurrent	Comments	MIB -1 %	Target	Voxel [Alanine]	Voxel MIB-1 %	LCModel SD %
1	Transitional	I	No	Fibrovascular Invasion	3.6%	High Ala	0.0129	0.80%	159%
2	Transitional	I	Yes			High Ala	0.0126	4.10%	125%
						Low Ala	0	N/A	999%
3	Transitional	I	No		1.7%	High Ala	0.0185	1.50%	70%
						Low Ala	0	2.90%	999%
4	Transitional	I	No		2.8%	Low Ala	0	7.30%	999%
						Low Ala	0	4.80%	999%
5	Atypical	II	No	With necrosis and clear cell	6.1%	High Ala	0.152	2.40%	14%
						Low Ala	0.00991	3.00%	159%
						High Cho	0.0057	1.80%	97%
						Low Cho	0.00491	2.70%	254%
6	Transitional	I	No		2.4%	High Ala	0.0136	1.70%	97%
						Low Ala	0	2.20%	999%
7	Meningothelial	I	No			High Ala	0.022	2%	74%
						Low Ala	0	3.1%	999%
8	Meningothelial	I	No	Dural Invasion		High Ala	0.0128	1.80%	94%
						Low Ala	0.0074	2%	173%
9	Fibrous	I	No		4.6%	High Ala	0.13	3.30%	11%
						Low Ala	0	1.90%	999%
10	Fibrous	I	No		<1%	Low Ala	0.00671	2.20%	358%
11	Spindle Cell	I	No			High Ala	0.136	15%	2.80%
						High Ala	0.259	10%	2.50%
12	Meningothelial	I	No	Fibrous bands	1-2%	High Ala	1.21	1.90%	50%
						Low Ala	0	1.50%	999%
13	Meningothelial	I	No		2.8%	High Ala	0.446	2.60%	19%
						Low Ala	0	4.00%	438%
14	Transitional	I	No		2.6%	High Ala	0.071	N/A	46%
						Low Ala	0.857	N/A	10%
15	Fibrous	I	No		1.8%	High Ala	1.037	1.70%	17%
						Low Ala	0	1.20%	999%

Table 2: Summary of Meningioma Subtype, Alanine Concentrations per Voxel and MIB-1%

Representative Cases

Patient 1:

A 39-year-old male developed a meningioma that was interpreted to be an atypical meningioma WHO Grade II. Features present during the pathological report were: transitional meningioma with predominately meningothelial features, streaming growth pattern, foci of active necrosis, sclerotic nodules. The tumor showed an overall MIB-1 index of 6.1% (Figure 2). Histology for region 1 (Figure 2B) showed a MIB-1 of 2.4% and appeared to be a higher grade than the tissue from region 2 (Figure 2C) on H & E. The tissue originating from region 1 had a low alanine concentration (Figure 2A spectra 1); therefore, a more aggressive part of the meningioma correlated with lower alanine concentration. Histology for region 2 showed a MIB-1 of 1.8% and was considered benign sample of meningioma correlated with elevated alanine concentration.

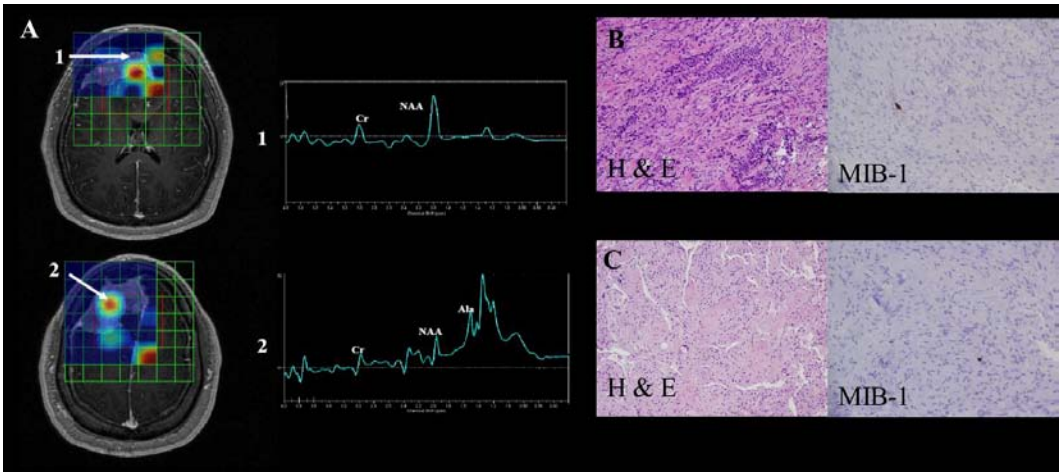

Figure 2: ***Patient 1:*** **A 39-year-old male developed a meningioma that was interpreted to be an atypical meningioma, WHO Grade II. Features cited in the pathological report were: transitional meningioma with predominately meningothelial features, streaming growth pattern, foci of active necrosis, sclerotic nodules. The tumor showed an overall MIB-1 index of 6.1%. A) Overlay of alanine (Ala) metabolite map on conventional MRI image. Numbers 1 and 2 refer to different tissue regions within the same meningioma. B) Region 1 showed a MIB-1 of 2.4% and appeared histologically to be of higher grade than tissue from region 2. H & E = hematoxylin & eosin. Tissue originating from region 1 had low Ala concentration (see accompanying spectra); therefore, a more aggressive part of the meningioma correlated with low alanine concentration. C) Region 2 showed a MIB-1 of 1.8% and was considered histologically benign. Correspondingly, Ala concentration was elevated.**

Patient 2

A 49 year old female developed a meningioma diagnosed as a meningothelial meningioma WHO Grade I, with sheet like growth pattern and focal necrosis. The overall MIB-1 value was 2.8% (Figure 3). Histology for region 1 (Figure 3B) showed a MIB-1 concentration of 2.6% demonstrating a more benign sample of meningioma that correlated with elevated alanine concentration. Histology for region 2 (Figure 3C) showed a MIB-1 of 4.0% showing a more aggressive part of the meningioma that correlated with low alanine concentration.

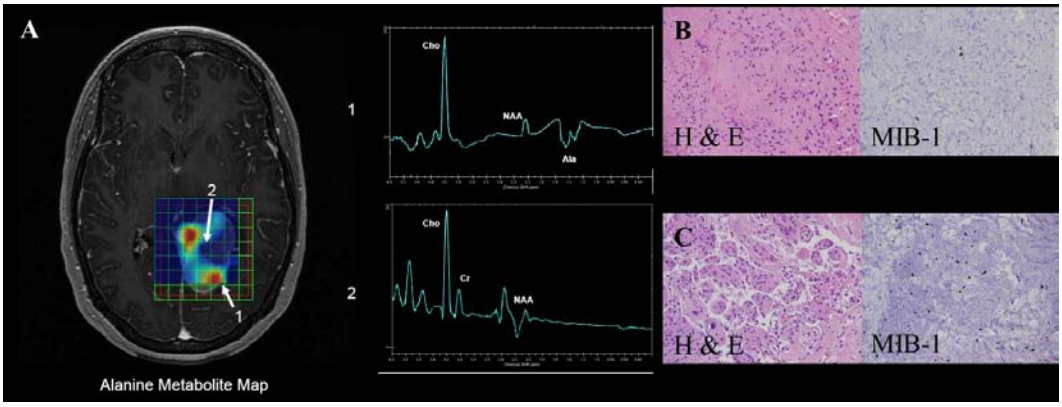

Figure 3: ***Patient 2:*** **A 49 year old female developed a meningioma diagnosed as a meningothelial meningioma, WHO Grade I, with sheet like growth pattern and focal necrosis. The overall MIB-1 value was 2.8%. A) Ala metabolite map overlaid on anatomical MR image shows regional variation in intratumoral Ala concentration. B) Region 1 showed a MIB-1 of 2.6% and a histologically benign region of meningioma with correspondingly elevated Ala concentration. C) Region 2 showed a MIB-1 of 4.0%, histological features of aggression, and correspondingly low Ala concentration.**

Ex vivo HR-MAS NMR versus *in vivo* 3D ^{1}H-MRSI spectra

HR-MAS NMR spectra showed reliable qualitative correlation with the *in vivo* 3D ^{1}H-MRSI spectra with 23 of 28 spectra demonstrating positive correlation (Table 3). Resonances for NAA, creatine, alanine, lactate, myo-Inositol and choline were found to be quantitatively comparable between the corresponding *in vivo* and *ex vivo* spectra (Figure 4).

Correlation Range	Number of Spectra Pairs	Interpretation
Correlation< -0.25	1	Weak Negative Association
-0.25<Correlation < 0.25	4	Little or No Association
0.25<Correlation<0.7	11	Weakly Positive Association
0.7<Correlation<0.9	4	Good Positive Association
0.9<Correlation<1.0	7	Strong Positive Association

Table 3: *Ex Vivo* HRMAS Spectra Versus *in vivo* ^{1}H-MRS spectra Pearson Correlation

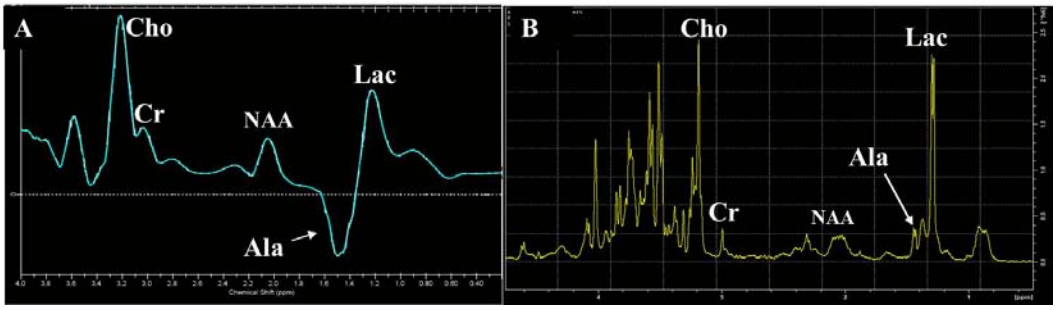

Figure 4: A) *In vivo* 3D ^{1}H-MRS voxel LCModel spectra prior to tissue resection. B) *Ex vivo* HR-MAS NMR voxel spectra of same tissue showing similar metabolite ratios. TE=144 demonstrate inverted Ala concentrations.

Meningioma Metabolites: Alanine

By the independent two-sample, two-tailed t-test, the mean of the maximum Alanine voxels biopsied in aggressive meningiomas is significantly lower than in non-aggressive meningiomas ($p=0.047$) (Figure 5). There were no statistically significant correlations between Alanine and MIB-1% (Figure 6). However, for every patient with a non-fibrous meningioma, the high Alanine voxel corresponded to a lower MIB-1%, while the low Alanine voxel corresponded with a high MIB-1%. For fibrous meningiomas, the opposite was true. Because of this difference between meningioma subtypes, there was no consistent statistical correlation between Alanine and MIB-1%.

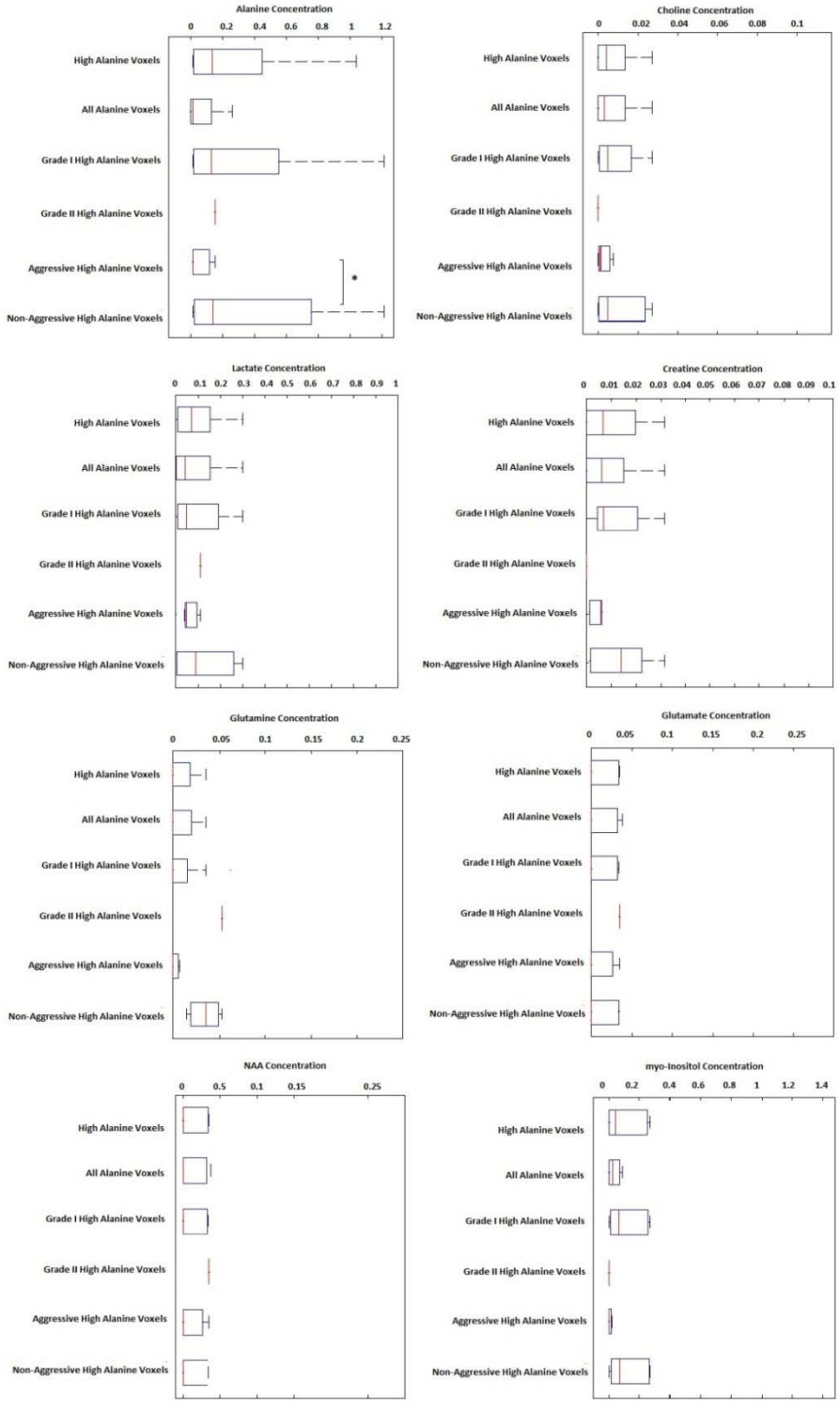

Figure 5: Mean concentrations of metabolites grouped according to clinical and pathological parameters. (* = P<0.05)

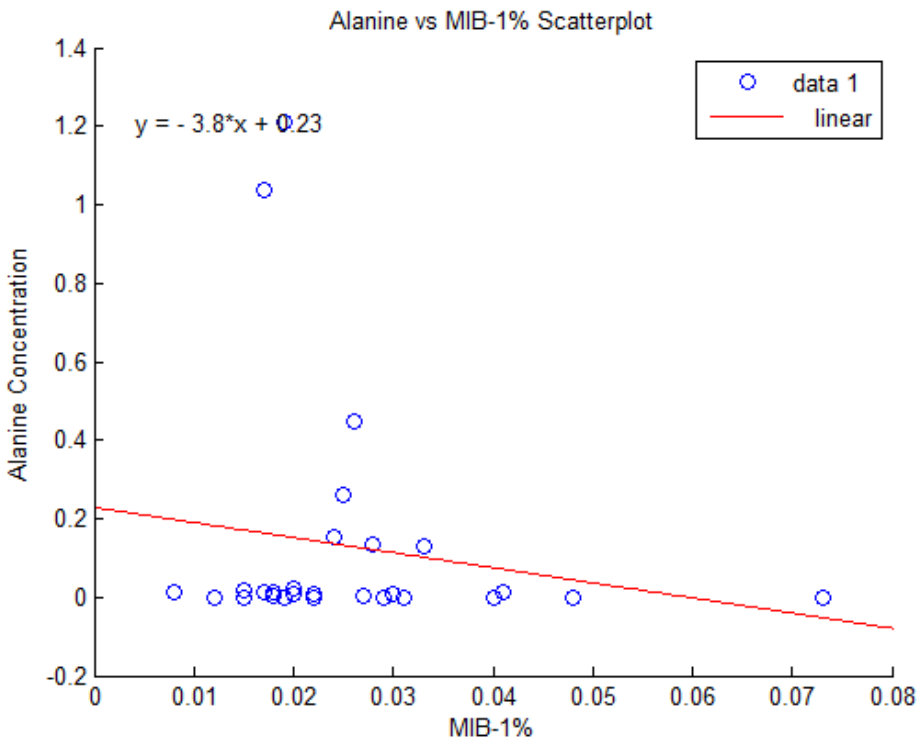

Figure 6: Alanine versus MIB-1% Scatterplot.

Other Metabolites

Choline, lactate, glutamine, and myo-inositol were found at lower concentrations within aggressive meningiomas, but these did not reach statistical significance. Two metabolites typically found in normal brain, creatine and NAA, did not demonstrate a significant change in concentration between aggressive and non-aggressive meningiomas.

Metabolite concentrations according to histological subtypes of meningioma

The metabolite concentrations across several different histological subtypes of meningioma were compared (Table 2). These results are summarized in Figure 7. Within the classical grade I subtypes of meningothelial, transitional, and spindle cell meningioma, we found regional heterogeneity in metabolite concentrations. These subtypes, as well as recurrent transitional meningioma and Grade II atypical meningiomas, demonstrated a negative relationship between alanine concentrations and MIB-1 percentages, i.e., more aggressive tissue corresponded to lower alanine concentrations and higher MIB-1. Interestingly, fibrous meningiomas and meningothelial with fibrous bands, which are also considered grade I tumors, were the only subtypes to demonstrate an opposite association: in these tumors, we found that increased alanine corresponded to higher MIB-1.

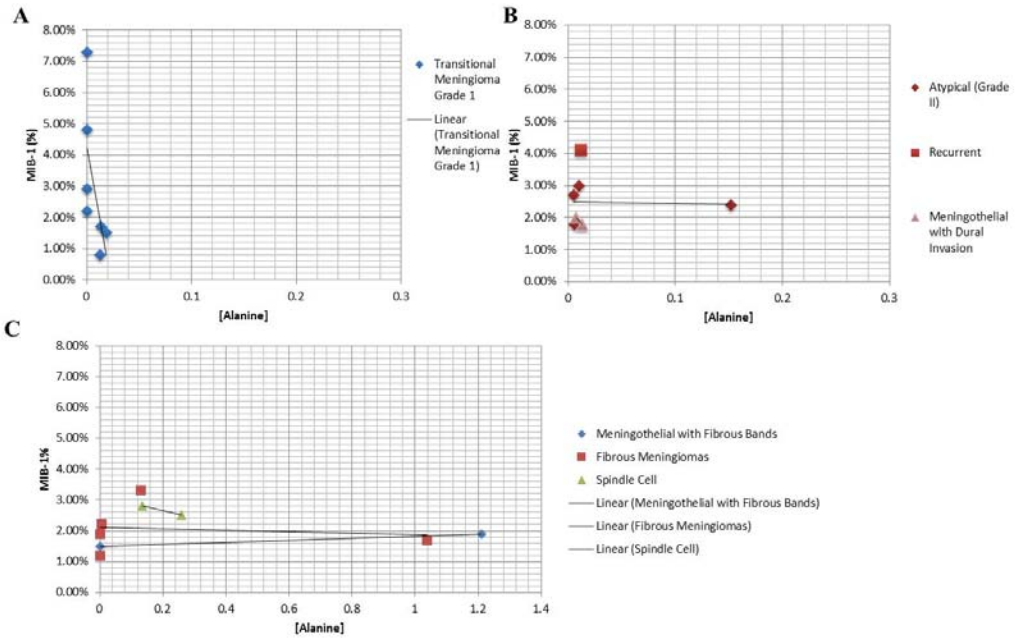

A) Transitional meningioma (Grade 1) showing decreased MIB-1 (%) with increased Ala concentration.
B) Atypical Meningioma (Grade II) and recurrent showing decreased MIB-1 (%) with increased Ala concentration.
C) Fibrous meningioma and meningothelial meningioma with fibrous bands demonstrating little to a slightly positive increased MIB-1 with increased Ala concentration in stark contrast to spindle cell with has a decreasing MIB-1% with an increasing Ala concentration.

Figure 7: Meningioma Subtypes: *In vivo* 3D ^{1}H-MRS Alanine concentration vs. MIB-1 (%).

Spatial variations in metabolite concentration

Inherent to 3D ^{1}H-MRSI is a proportional decrease in metabolite concentrations from the isocentric point of the ROI due to intensity nonuniformity as has been observed in phantom studies.[33] In spite of this limitation, we still found a consistent, stereotyped variation in metabolite concentration between the center and periphery of grade I, but not higher grade, meningiomas. In grade I tumors, the periphery showed increased alanine concentration while the tumor center showed increased choline concentration (Figure 8a and 8b). In addition, lactate increased slightly in the center (Figure 8c). Though the trends were present none of the metabolites had a statistically significant difference.

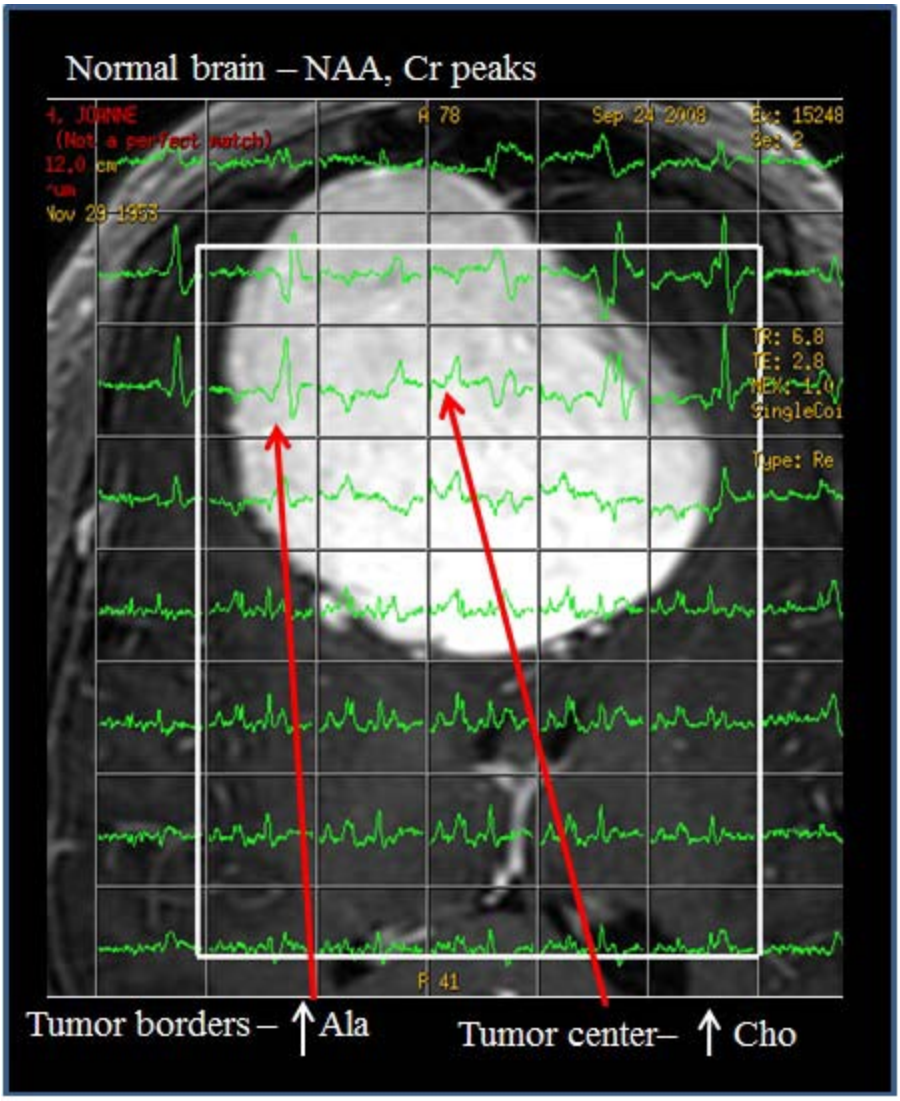

Figure 8a: Functool Image of ROI Slice Showing Regional Heterogeneity of a Grade I Meningioma. Increase Alanine concentration is seen at periphery of tumor. Increased Choline is seen in center of tumor and normal brain spectra are found with representative NAA and Cr peaks.

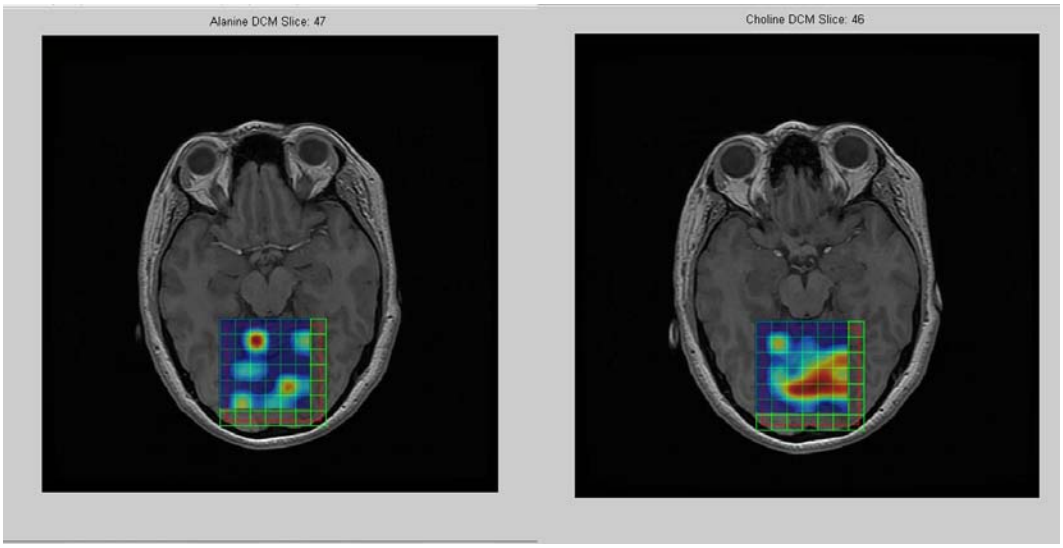

Figure 8b: Metabolite map for alanine and choline demonstrating metabolite concentration differences in peripheral versus central regions of a grade I meningioma.

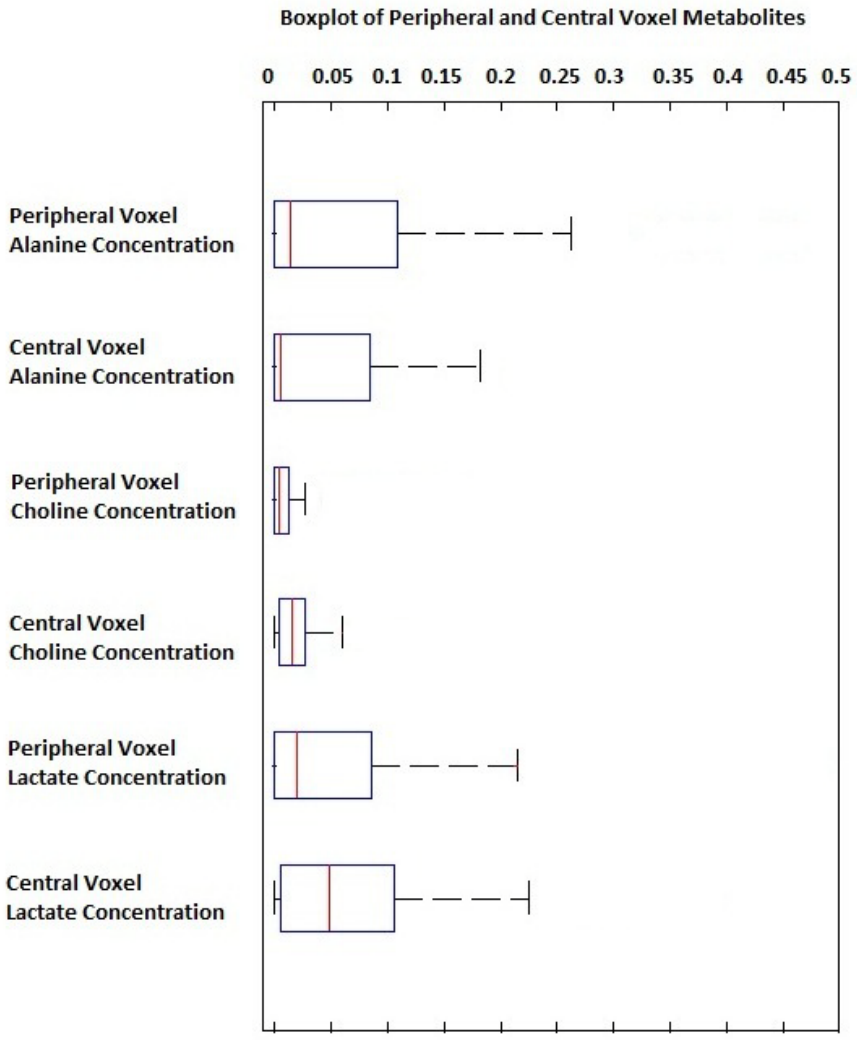

Figure 8c: Metabolite concentration differences in the periphery versus center of Grade I Meningioma (*, P<0.05).

3D ^{1}H-MRSI spectra versus 1D ^{1}H-MRS spectra

In addition to the 3D ^{1}H-MRSI spectra, 1D ^{1}H-MRS spectra were also obtained during the same exams for comparison, given the greater widespread use of single voxel MRS. In the majority of tumors, the 1D spectra matched the overall trends of the 3D spectra. Of particular interest, in one of the patients with sphenoid wing meningioma the 1D MRS spectra was not usable due to unsuppressed water signal, but the 3D acquisition in the same location was able to generate clear usable data (Figure 9).

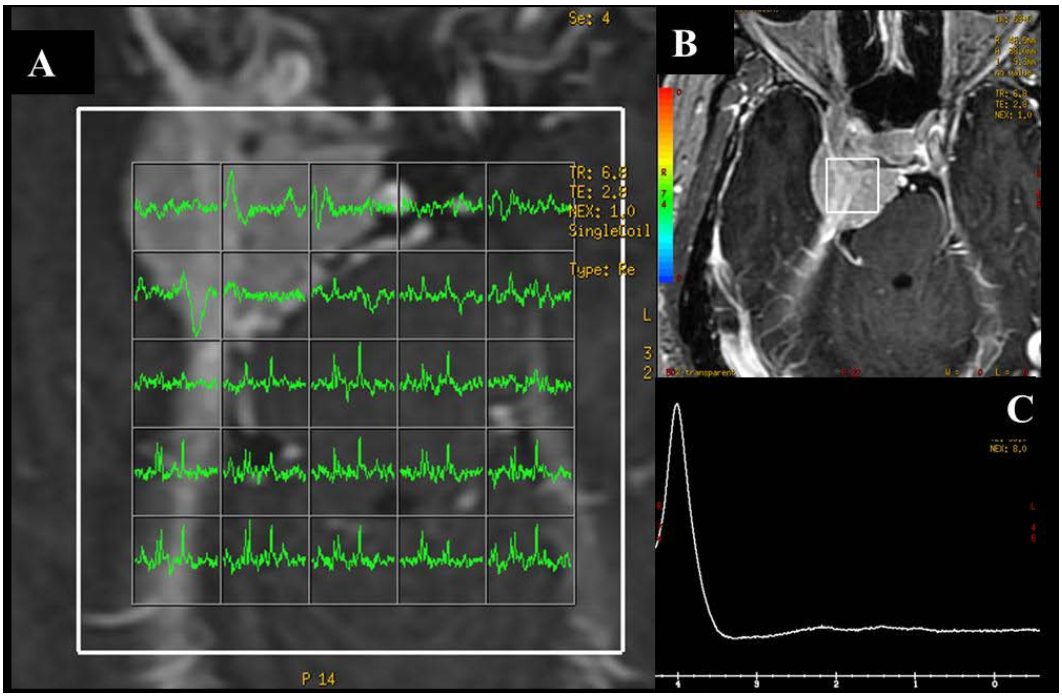

Figure 9: 3D ^{1}H-MRS vs. 1D ^{1}H-MRS spectra in sphenoid wing meningioma. A) Functool image of ROI slice through meningioma showing very clear usable spectra inside of tumor and in normal brain. B) Functool image of ROI for 1D ^{1}H-MRS inside meningioma. C) Spectra from 1D ^{1}H-MRS showing large unsuppressed water peak and unusable spectra.

Discussion

In this study, we have used a non-invasive imaging technique, 3D ^{1}H-MRSI, to confirm regional heterogeneity within meningiomas, and, further, to identify metabolites which are associated with tissue areas indicating histological and immunohistochemical markers of

aggression. Conventional imaging modalities are presently unable to predict which meningiomas are likely to recur. With the five-year survival rate for aggressive meningiomas differing dramatically from benign tumors (65% for grade III compared to 90-91% for grade I), it is important to identify tumors that should be treated up front with adjuvant therapies.[9,10,13,17,20] Histology is the current gold standard for grading meningiomas and assessing their potential for recurrence, but is limited by sampling error and the fact that even benign meningiomas may contain regions with more invasive potential.[23-25]

Using 3D 1H-MRSI in an integrated, multimodal, image guided surgery system

^{1}H-MRS is a non-invasive imaging modality that allows insight into intratumoral metabolic function. With the recent emergence of multivoxel 3D ^{1}H-MRSI techniques, frequently an entire tumor volume can be examined in relatively small voxel units, and the concentration of several metabolites determined within each voxel. We have shown that 3D ^{1}H-MRSI can highlight key regions within meningiomas which, on the basis of their metabolic profiles, should be targeted for

biopsy when complete resection is unsafe or technically prohibitive. Previous 2D ^{1}H-MRSI techniques required multiple scans to obtain the same volumetric coverage, with associated increased scan time and cost. 3D ^{1}H-MRSI generates more symmetrically shaped voxels through the ROI compared to 2D ^{1}H-MRSI, although this may require significant software and hardware upgrades to existing MRI systems. Additionally, and curiously, our experience suggests that 3D may be superior to 1D ^{1}H-MRS techniques in imaging tumors near the skull base such as complex areas like the sphenoid wing which were previously considered inaccessible to spectroscopic imaging (Figure 8). Further experience with 3D ^{1}H-MRSI near the skull base will need to be obtained in order to confirm this phenomenon.

We attempted to develop a scanning protocol that could be used in a busy MRI department. Scan time was determined to fit into normal scanner allotment times. LCModel output was generated for scans that would mirror the one time run typical of clinical MRI acquisition. Though the spectra could have been made even more clean, the ex vivo HRMAS comparison with the in vivo MRS data shows that the data generated from the clinical MRI department optimized patient scan time is sufficient to generate useful data.

Integrating 3D ^{1}H-MRSI data into IGS systems offers a new opportunity to exploit the full potential of non-invasive spectroscopic imaging. In our study, the STEALTH IGS system integrated with 3D ^{1}H-MRSI allowed the surgeon to prospectively select voxels of interest for biopsy, and was as straightforward to use as when other imaging modalities are integrated, e.g., perfusion MR or positron emission tomography. The integration into a standard neurosurgical IGS platform is crucial because surgeons are very familiar with the interface and the MRS image data is simply interacted with as any other imaging modality. In addition, the acquisition of 3D ^{1}H-MRSI added relatively little time to the pre-operative imaging sequences, while adding a dimension of metabolic information intra-operatively. Reliability of the 3D ^{1}H-MRSI spectra are high, as spectral characteristics correlate with *ex vivo* HR-MAS spectra, histological and immunohistochemical analyses, and our previous NMR and molecular studies of *ex vivo* meningioma tissue. The application to a clinical setting was a logical translational step in furthering the use of metabolic imaging data in the management of meningiomas. The small subset of samples that had differences between *in vivo* 3D ^{1}H-MRSI and *ex vivo* HR-MAS may be due to brain shift before resection,

degeneration of tissue during processing for HR-MAS analysis, or a different concentration of metabolites even within the small portion of tissue partitioned from the voxel sample.

Decreased alanine: a marker of histological aggression?

We hypothesized and found that regions of decreased alanine concentration, as demonstrated *in vivo* using 3D ^{1}H-MRSI, corresponded to regions of increased histological aggression. This finding is in agreement with recent *ex vivo* studies from our group where decreased alanine concentration corresponded to higher tumor grade and increased likelihood of recurrence.[24,26] In contrast, we found that within individual tumors higher alanine concentrations correlated with lower MIB-1 percentages. Currently, a MIB-1 of 2% or more is considered consistent with a higher tumor grade.[20] With a larger sample size, it is reasonable to hypothesize that a 2% cut-off will predict a statistically significant difference, allowing surgeons to very accurately target tumor tissue at increased risk of recurrence. Of course, MIB-1 is but one marker of tumor aggression, and we plan to do further chromosomal genomic hybridization (CGH) analysis of

tumor samples to compare alanine as well as the entire body of metabolite concentrations with known genetic markers of increased aggression.

In most of our patients, the MIB-1 index of the overall tumor was actually higher than sampled voxels showing low alanine. We attribute this to the fact that the pathologists typically examine tissue from the large core of the meningioma. Our principal focus was to define the MIB-1 basis for voxels highest in alanine along with a selection of some of the voxels that were of lower alanine intensity. Often, these voxels were in neighboring locations which provided ease in resection and was used as an attempt to define subtle differences in histology accompanied by similarly subtle differences in biochemistry.

The exact role of alanine in the metabolic processes of meningiomas is unknown. Meningiomas appear to have alanine as a "normal" part of their metabolism. Indeed the tissues they originate from show high alanine concentrations (from our experience of MRS of swine dura, unpublished). Alanine reciprocally generates pyruvate in the glycolytic pathway through the function of alanine aminotransferase. In anaplastic meningiomas, it has been shown that

lactate dehydrogenase function is greatly elevated signifying the increased production of pyruvate from lactate.[8] It is possible that the decrease in alanine in recurrent or more aggressive meningiomas results from increased functioning of alanine aminotransferase to increase pyruvate production to fuel the Krebs Cycle, inducing greater aggression and divergence from the pathway of "normal" meningioma metabolism. Additionally, high alanine concentrations have been shown to inhibit the MII-type pyruvate kinase found in meningiomas but not normal brain.[38,39] The high alanine found in non-aggressive meningiomas may serve to inhibit growth in these tumors by limiting glycolytic formation of pyruvate.

While other metabolites demonstrated changes within more aggressive meningiomas and may also be helpful in preoperative grading, alanine is ideal because it is a metabolite uniquely associated with meningiomas. At this stage we could not target other metabolites and their distributions for prospective sampling due to constraints related to operative time. Other metabolites deserve further investigation.

Spatial variations in metabolite concentration and biological behavior

We found general stereotyped differences in the overall concentrations of metabolites within the tumor periphery versus the core. Though not significantly different with the current sample size of patients, an increased number of patients that may continue to show the same trends could lead to significance. In grade I meningiomas, higher alanine concentrations were found in the periphery of the tumor. Higher resonances for choline were found in the more central portions of the Grade I tumor, perhaps indicating increased cellularity or cell turn over. These metabolic characteristics may indicate that the outer parts of a meningioma are more "meningioma normal" (less aggressive) and the central portions are more aggressive or divergent from the usual meningioma metabolic profile.

We have noted the peripheral distribution of alanine in other studies, however, the 3D ^{1}H-MRSI technique employed in this study allowed us to observe it more systematically and in more detail in humans.[28,29,31] This distribution of higher alanine concentrations found primarily at the periphery of lower grade meningioma may explain why meningiomas remain quiescent after surgery, i.e., the more aggressive, central portion of the meningioma has been removed, while the less aggressive peripheral tissue or cell remnants adherent

to the dura or other attaching structures remain. Alanine is not detected in brain tissue with our sequence, and thus any alanine observed in peripheral voxels of partial volume with brain tissue is deemed to originate from meningioma tissue alone.

The relationship between metabolic signature and histological subtype

The relationship between lower alanine concentration and increased histological aggressiveness held across all histological subtypes of meningioma except the fibrous (also known as fibroblastic) subtype. Fibrous meningiomas have been found to have an increased amount of type IV collagen compared to other meningioma subtypes.[21,39] Alanine has been associated with Type IV collagenous tissue and in the fibronectin-like collagen-binding domain synthesis of type IV collagen.[3,5] Consequently, the distinct composition of the fibrous subtype may explain differences in the direction of changes in alanine concentration compared to other subtypes. In any case, fibrous meningiomas are classified as grade I and are considered distinctly

unlikely to recur[9], implying that the role of MRS in detecting regions of histological aggression may be less important in this tumor subtype. Furthermore, diffusion tensor imaging, T2 reversed MRI, and perfusion MRI have all shown promise in differentiating fibroblastic meningiomas from other subtypes.[35,42,43] Further study will continue to shed light on the characteristic metabolic patterns within various subtypes of meningioma.

3D ^{1}H-MRSI to optimize surgical resection and inform adjuvant therapy

Meningiomas pose some of the most challenging scenarios encountered in operative neurosurgery. Tumors located in or near the sphenoid wing, olfactory groove, venous sinuses, cerebello-pontine angle, and cranial nerves serve can be considerable tests of the experience and skill of the neurosurgeon. The main advantage of 3D ^{1}H-MRSI integrated into IGS is in brain tumor scenarios where a complete resection is impossible. 3D ^{1}H-MRSI may at least guide the surgeon to more aggressive areas of the tumor which he/she should attempt to remove, or at the very least biopsy.

Frequently, meningioma operations result in subtotal resections in these areas with the question of the need for adjuvant therapy. Imaging techniques such as 3D ^{1}H-MRSI, if routinely incorporated into IGS systems as we have done here with the STEALTH system, may indicate whether the tumor is likely to behave aggressively or recur, and may help decide whether adjuvant therapy should be used or whether more aggressive targeted resection is warranted. The question of adjuvant therapy with regard to meningiomas remains controversial. At present, many subtotally resected grade I meningiomas do not receive any adjuvant therapy: residual tumor is simply watched with serial imaging and only treated further if it shows growth. This study, however, indicates the feasibility for 3D ^{1}H-MRSI to show aggressive areas within meningiomas and perhaps can be used to examine the growth potential of residual tumor tissue[28], as noted by our successful examination into the dura of a very low lying tumor along the sphenoid ridge (Figure 8). We have begun larger prospective studies to elucidate the relationships between meningioma metabolism, importance of surgical resection, and need for adjuvant therapy.

Conclusion

Alanine, detected non-invasively using 3D ^{1}H-MRSI, is associated with aggressive histological features and inversely associated with levels of MIB-1 Ki67 within meningioma tissue. There is regional heterogeneity in the concentrations of these markers within individual tumors. Furthermore, 3D ^{1}H-MRSI can exploit these regional differences to separate more aggressive from less aggressive areas within a given meningioma. This knowledge may be useful to the neurosurgeon faced with the task of meningioma resection and in the planning adjuvant therapy for residual meningioma tissue following subtotal removal.

References

1. Abramovich, C. M. and R. A. Prayson (1999). "Histopathologic features and MIB-1 labeling indices in recurrent and nonrecurrent meningiomas." Arch Pathol Lab Med 123(9): 793-800.
2. Ala-Korpela, M., P. Posio, S. Mattila, A. Korhonen and S. R. Williams (1996). "Absolute quantification of phospholipid metabolites in brain-tissue extracts by 1H NMR spectroscopy." J Magn Reson B 113(2): 184-9.
3. Baboonian, C., P. J. Venables, D. G. Williams, R. O. Williams and R. N. Maini (1991). "Cross reaction of antibodies to a glycine/alanine repeat sequence of Epstein-Barr virus nuclear antigen-1 with collagen, cytokeratin, and actin." Ann Rheum Dis 50(11): 772-5.
4. Commins, D. L., R. D. Atkinson and M. E. Burnett (2007). "Review of meningioma histopathology." Neurosurg Focus 23(4): E3.
5. Collier, I. E., P. A. Krasnov, A. Y. Strongin, H. Birkedal-Hansen and G. I. Goldberg (1992). "Alanine scanning mutagenesis and functional analysis of the fibronectin-like collagen-binding

domain from human 92-kDa type IV collagenase." J Biol Chem 267(10): 6776-81.

6. Govindaraju, V., K. Young and A. A. Maudsley (2000). "Proton NMR chemical shifts and coupling constants for brain metabolites." NMR Biomed 13(3): 129-53.
7. Henn, W., S. Urbschat. *Monosomy 1p is correlated with enhanced in vivo glucose metabolism in meningiomas.* Cancer Genet Cytogenet, 1995. **79**(2): p. 144-8.
8. Herting, B., J. Meixensberger, W. Roggendorf and H. Reichmann (2003). "Metabolic patterns in meningiomas." J Neurooncol 65(2): 119-23.
9. Ildan, F., T. Erman, A. I. Gocer, M. Tuna, H. Bagdatoglu, E. Cetinalp and R. Burgut (2007). "Predicting the probability of meningioma recurrence in the preoperative and early postoperative period: a multivariate analysis in the midterm follow-up." Skull Base 17(3): 157-71.
10. Ko, K. W., D. H. Nam, D. S. Kong, J. I. Lee, K. Park and J. H. Kim (2007). "Relationship between malignant subtypes of meningioma and clinical outcome." J Clin Neurosci 14(8): 747-53.

11. Lanzafame, S., A. Torrisi, G. Barbagallo, C. Emmanuele, N. Alberio and V. Albanese (2000). *Correlation between histological grade, MIB-1, p53, and recurrence in 69 completely resected primary intracranial meningiomas with a 6 year mean follow-up*. Pathol Res Pract, 2000. **196**(7): p. 483-8.
12. Lehnhardt, F. G., G. Rohn, R. I. Ernestus, M. Grune and M. Hoehn (2001). "1H- and (31)P-MR spectroscopy of primary and recurrent human brain tumors in vitro: malignancy-characteristic profiles of water soluble and lipophilic spectral components." NMR Biomed 14(5): 307-17.
13. Mahaley, M.S., Jr., C. Mettlin, N. Natarajan, E. R. Laws, Jr., B.B. Peace(1989). *National survey of patterns of care for brain-tumor patients.* J Neurosurg, 1989. **71**(6): p. 826-36.
14. Maillo, A., P. Diaz, J.M. Sayagues, A. Blanco, M.D. Tabernero, J. Ciudad,A. Lopez, J.M.Goncalves and A. Orfao (2001). *Gains of chromosome 22 by fluorescence in situ hybridization in the context of an hyperdiploid karyotype are associated with aggressive clinical features in meningioma patients.* Cancer, 2001. **92**(2): p. 377-85.
15. Majos, C., J. Alonso, C. Aguilera, M. Serrallonga, J. Perez-

Martin, J. J. Acebes, C. Arus and J. Gili (2003). "Proton magnetic resonance spectroscopy ((1)H MRS) of human brain tumours: assessment of differences between tumour types and its applicability in brain tumour categorization." Eur Radiol 13(3): 582-91.

16. Majos, C., M. Julia-Sape, J. Alonso, M. Serrallonga, C. Aguilera, J. J. Acebes, C. Arus and J. Gili (2004). "Brain tumor classification by proton MR spectroscopy: comparison of diagnostic accuracy at short and long TE." AJNR Am J Neuroradiol 25(10): 1696-704.
17. McCarthy, B.J., et al., *Factors associated with survival in patients with meningioma.* J Neurosurg, 1998. **88**(5): p. 831-9.
18. McLean, M.A., F.G. Woermann, G.J. Barker and J.S. Duncan (2000). "Quantitativeanalysis of short echotime (1)H-MRSI of cerebral gray and white matter. " Magn Reson Med 44(3): 201-11.
19. Monleon, D., J. M. Morales, J. Gonzalez-Darder, F. Talamantes, O. Cortes, R. Gil-Benso, C. Lopez-Gines, M. Cerda-Nicolas and B. Celda (2008). "Benign and atypical meningioma metabolic signatures by high-resolution magic-angle spinning molecular

profiling." J Proteome Res 7(7): 2882-8.

20. Nakasu, S., T. Fukami, J. Jito and K. Nozaki (2009). "Recurrence and regrowth of benign meningiomas." Brain Tumor Pathol 26(2): 69-72.

21. Ogawa, K., M. Oguchi, Y. Nakashima and H. Yamabe (1989). "Distribution of collagen type IV in brain tumors: an immunohistochemical study." J Neurooncol **7**(4): 357-66.

22. Perry, A., S.L. Stafford, B.W. Scheithauer, V.J. SUman and C.M. Lohse (1997). *Meningioma grading: an analysis of histologic parameters.* Am J Surg Pathol, 1997. **21**(12): p. 1455-65.

23. Pfisterer, W. K., S. W. Coons, F. Aboul-Enein, W. P. Hendricks, A. C. Scheck and M. C. Preul (2008). "Implicating chromosomal aberrations with meningioma growth and recurrence: results from FISH and MIB-I analysis of grades I and II meningioma tissue." J Neurooncol 87(1): 43-50.

24. Pfisterer, W. K., W. P. Hendricks, A. C. Scheck, R. A. Nieman, T. H. Birkner, W. W. Krampla and M. C. Preul (2007). "Fluorescent in situ hybridization and ex vivo 1H magnetic resonance spectroscopic examinations of meningioma tumor tissue: is it possible to identify a clinically-aggressive subset of benign

meningiomas?" Neurosurgery 61(5): 1048-59; discussion 1060-1.

25. Pfisterer, W. K., N. C. Hank, M. C. Preul, W. P. Hendricks, J. Pueschel, S. W. Coons and A. C. Scheck (2004). "Diagnostic and prognostic significance of genetic regional heterogeneity in meningiomas." Neuro Oncol 6(4): 290-9.

26. Pfisterer, W. K., R. A. Nieman, A. C. Scheck, S. W. Coons, R. F. Spetzler and M. C. Preul (2010). "Using ex vivo proton magnetic resonance spectroscopy to reveal associations between biochemical and biological features of meningiomas." Neurosurg Focus 28(1): E12.

27. Pietruszka, M., H. Salazar, and C. Pena, *Malignant meningioma: ultrastructure and observations on histogenesis.* Pathology, 1978. **10**(2): p. 169-73.

28. Preul, M. C., Z. Caramanos, R. Leblanc, J. G. Villemure and D. L. Arnold (1998). "Using pattern analysis of in vivo proton MRSI data to improve the diagnosis and surgical management of patients with brain tumors." NMR Biomed 11(4-5): 192-200.

29. Preul, M. C., Z. Caramanos, D. L. Collins, J. G. Villemure, R. Leblanc, A. Olivier, R. Pokrupa and D. L. Arnold (1996). "Accurate, noninvasive diagnosis of human brain tumors by

using proton magnetic resonance spectroscopy." Nat Med 2(3): 323-5.

30. Ratai, E. M., S. Pilkenton, M. R. Lentz, J. B. Greco, R. A. Fuller, J. P. Kim, J. He, L. L. Cheng and R. G. Gonzalez (2005). "Comparisons of brain metabolites observed by HRMAS 1H NMR of intact tissue and solution 1H NMR of tissue extracts in SIV-infected macaques." NMR Biomed 18(4): 242-51.
31. Sankar, T., R. Assina, J. P. Karis, N. Theodore and M. C. Preul (2008). "Neurosurgical implications of mannitol accumulation within a meningioma and its peritumoral region demonstrated by magnetic resonance spectroscopy: case report." J Neurosurg 108(5): 1010-3.
32. Sibtain, N. A., F. A. Howe and D. E. Saunders (2007). "The clinical value of proton magnetic resonance spectroscopy in adult brain tumours." Clin Radiol 62(2): 109-19.
33. Sled, J. G., A. P. Zijdenbos and A. C. Evans (1998). "A nonparametric method for automatic correction of intensity nonuniformity in MRI data." IEEE Trans Med Imaging 17(1): 87-97.
34. Smith, S. J., S. Boddu and D. C. Macarthur (2007). "Atypical

meningiomas: WHO moved the goalposts?" Br J Neurosurg 21(6): 588-92.

35. Tropine, A., P. D. Dellani, M. Glaser, J. Bohl, T. Ploner, G. Vucurevic, A. Perneczky and P. Stoeter (2007). "Differentiation of fibroblastic meningiomas from other benign subtypes using diffusion tensor imaging." J Magn Reson Imaging 25(4): 703-8.
36. Tugnoli, V., L. Schenetti, A. Mucci, F. Parenti, R. Cagnoli, V. Righi, A. Trinchero, L. Nocetti, C. Toraci, L. Mavilla, G. Trentini, E. Zunarelli and M. R. Tosi (2006). "Ex vivo HR-MAS MRS of human meningiomas: a comparison with in vivo 1H MR spectra." Int J Mol Med 18(5): 859-69.
37. US, C.B.T.R.O.T., *2004-2006 Primary Brain Tumors in the United States.* 2009: p. 19.
38. van Veelen, C. W., G. E. Staal, H. Verbiest and A. M. Vlug (1977). "Alanine inhibition of pyruvate kinase in gliomas and meningiomas. A diagnostic tool in surgery for gliomas?" Lancet 2(8034): 384-5.
39. van Veelen, C. W., H. Verbiest, A. M. Vlug, G. Rijksen and G. E. Staal (1978). "Isozymes of pyruvate kinase from human brain, meningiomas, and malignant gliomas." Cancer Res 38(12): 4681-7.

40. Willis, J., C. Smith, J. W. Ironside, S. Erridge, I. R. Whittle and D. Everington (2005). "The accuracy of meningioma grading: a 10-year retrospective audit." Neuropathol Appl Neurobiol 31(2): 141-9.
41. Xu, M., J. Ye, D. Yang, X. Xu, T. T. Yeo, W. H. Ng and C. C. Lim (2007). "Ex-vivo NMR of unprocessed tissue in water: a simplified procedure for studying intracranial neoplasms." Anal Bioanal Chem 389(7-8): 2153-9.
42. Yoneoka, Y., Y. Fujii, H. Takahashi and T. Nakada (2002). "Pre-operative histopathological evaluation of meningiomas by 3 0T T2R MRI." Acta Neurochir (Wien) **144**(10): 953-7; discussion 957.
43. Zhang, H., L. A. Rodiger, T. Shen, J. Miao and M. Oudkerk (2008). "Preoperative subtyping of meningiomas by perfusion MR imaging." Neuroradiology 50(10): 835-40.

3D ^{1}H-MR Spectroscopy Integrated into a Standard Neurosurgical Image Guidance System: Providing a Resection Advantage and Determining Biochemical Markers of Clinically Aggressive Meningiomas *In Vivo*

Nina Z. Moore, MS, Mark C. Preul, MD

Barrow Neurological Institute Neurosurgery Research Laboratory

Introduction

Meningiomas comprise 1/3 of brain tumors. Though they are often considered benign, even benign meningiomas can behave aggressively.

Treatment differs based on grade and behavior:

Grade I: no treatment or surgery alone and MRI follow up

Grade II/III or aggressive behavior: surgery + adjuvant therapy

Currently, grade is dependent on histology after surgery. Knowledge of grade prior to surgery would allow an advantage in resection and treatment of the tumors.

^{1}H-MR Spectroscopy (^{1}H-MRS) evaluates metabolite levels and can differentiate tumor types as well as quantify tumor metabolism.

High alanine (Ala) concentration in meningiomas can differentiate it from other CNS tumors using ^{1}H-MRS.

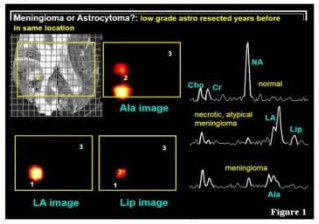

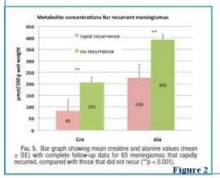

Ex vivo tissue analysis in NMR evaluation showed a correlation between **decreased alanine** levels within meningiomas and more **aggressive** meningiomas

Pfisterer, et al., 2007.

Hypotheses

- *In vivo* multi-voxel 3D ^{1}H-MRS data can be used intraoperatively with coregistration on STEALTH neuronavigation system
- *In vivo* multi-voxel 3D ^{1}H-MRS can detect regional biochemical alterations unique to clinically aggressive meningiomas and can correlate *ex vivo* results
- *In vivo* multi-voxel 3D ^{1}H-MRS integrated with IGS can provide a meningioma resection advantage, or allow metabolically-guided selection of tissue sampling for study

Methods

27	**PATIENTS SCANNED**	
	18	**primary meningiomas with tissue collected**
	1	**recurrent meningioma with tissue collected**
	3	**not meningiomas**
	1	**moved head during MRS acquisition**
	2	**severely claustrophobic**
	2	**no operation**
19	**3-D ^{1}H-MRS data sets examined with SAGE/LCModel**	
	15	**sets with quantifiable metabolites, areas of interest identified within tumor and selected for resection**
	4	**sets discarded – inadequate water suppression or voxel placement prevented analysis**

Methods

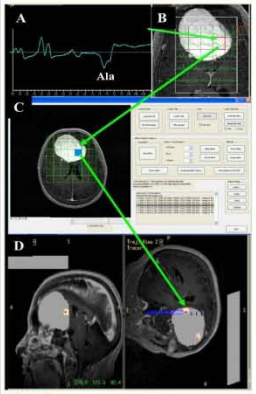

1. Newly diagnosed and recurrent meningioma patients are scanned preoperatively with a 3T GE Signa scanner

   3D CSI ^{1}H-MRS is performed immediately after the pre-operative MRI STEALTH intraoperative navigation "wand" scan sequence, avoiding placement of the excitation voxel over the skull base, bone and scalp

2. The 3D MRS spectral data is quantified using GE's Sage software and LCModel (Provencher) (Figure A)

3. Voxels of interest are selected based on presence or absence of alanine, lactate, choline and creatinine (Figure B: highlighted in red)

4. Selected voxels are entered into our MATLAB software GUI to create a STEALTH overlay (Figure C)

5. Neurosurgeons resect the voxels of interest using image guidance system (Figure D: blue arrow showing intra-operative identification of the voxel of interest)

6. Histology and MIB-1 indexing of tumor samples was performed

7. NMR High Resolution Magic Angle Spinning (HRMAS) was performed on resected tissue to compare *ex vivo* spectra to the corresponding *in vivo* ^{1}H-MRS spectra and evaluate the STEALTH integrated overlay technique

Results

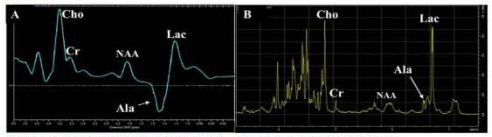

Figure 4 LCModel Spectra from Patient Voxel A HR-NMR Spectra for Patient Voxel A

Figure 4: Image Guidance System overlay greatly enhances the accuracy of resecting the voxels of interest. ^{1}HR-MAS NMR spectra showed qualitatively reliable correlation with the *in vivo* ^{1}H-MRS spectra with 23 of 28 spectra matching.

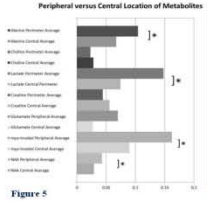

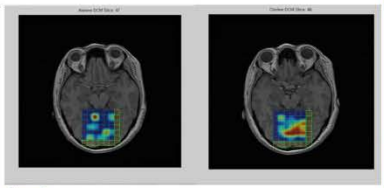

Figures 5 and 6: 14 grade I tumor **periphery** showed **increased Alanine** concentrations ($p<.05$). Tumor **centers** showed **increased Cho** concentrations and **decreased Alanine** concentrations.

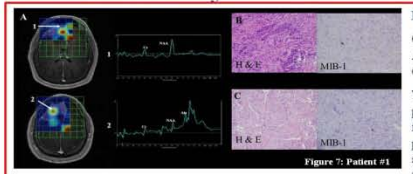

Figure 7: Patient #1

Overall Pathology Report: Atypical Meningioma WHO Grade II

Transitional meningioma with predominately meningothelial features, streaming growth pattern, foci of active necrosis, sclerotic nodules. MIB-1 6.1%

Histology for Sample 1 showed a MIB-1 of 2.4% but appeared to be a higher grade than the Sample 2 on H & E; therefore, a more **aggressive** part of the meningioma that correlated with **low alanine** concentration.

Histology for Sample 2 showed a MIB-1 of 1.8% and was considered **benign** sample of meningioma that correlated with **elevated alanine concentration**.

Figure 8: Patient #2

Overall Pathology Report: Meningothelial Meningioma WHO Grade 1

Sheet like growth pattern and focal necrosis. MIB-1 value of 2.8%

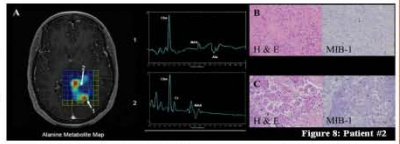

Histology for Sample 1 showed a MIB-1 concentration of 2.6% demonstrating a more **benign** sample of meningioma that correlated with **elevated alanine concentration**.

Histology for Sample 2 showed a MIB-1 of 4.0% showing a more **aggressive** part of the meningioma that correlated with **low alanine** concentration.

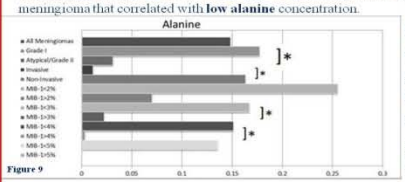

Figure 9: Alanine concentration is decreased in areas of higher MIB-1% meningioma for both grade I and grade II ($p<.05$)

Conclusions

- *In vivo* multi-voxel 3D ^{1}H-MRS detects regional biochemical alterations showing that meningiomas have regionally heterogeneous metabolite distribution.
- *In vivo* multi-voxel 3D ^{1}H-MRS data can be overlayed on the STEALTH neuronavigation system to accurately biopsy and resect areas of interest.
- 3D ^{1}H-MRS spectra correlate with *ex vivo* ^{1}HR-MAS NMR spectra
- ^{1}H-MRS alanine concentration may predict tumor recurrence.

Funding:
AANS Medical Student Summer Research Fellowship, BNF